Food Hydrocolloids 142 (2023) 108806

Contents lists available at ScienceDirect

Food Hydrocolloids

journal homepage: www.elsevier.com/locate/foodhyd

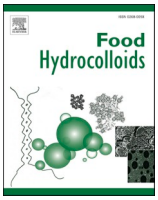

Formation and physicochemical properties of insoluble complexes resulted from high methoxyl pectin – protein interactions

Marianthi Zioga, Vasiliki Evageliou *

Department of Food Science and Human Nutrition, Agricultural University of Athens, 75 IeraOdos, 11855, Athens, Greece

ARTICLE INFO

Keywords:
Complexes
Pectin
Sodium caseinate
Whey protein isolate
Pea protein isolate

ABSTRACT

The present work studied the complex coacervation of high methoxyl pectin (HMP) with three proteins [Whey protein isolate (WPI), Sodium caseinate (SC) or pea protein isolate (PPI)] during acidification. Each protein and HMP were mixed at various ratios (1:1 to 10:1) with the sum of their concentrations ranging from 0.2 to 1.1%. Complex coacervate formation, as investigated by phase diagrams and zeta potential measurements, depended on the protein and the strength of the electrostatic protein-HMP interactions. Optimum coacervation was achieved at 6:1 mixing ratio and at pH 4 for SC and WPI or pH 3 for PPI. The complexes formed at these conditions were isolated and studied further in terms of their colour, moisture content, solubility, pH, conductivity, kinematic viscosity, density, porosity, flowability and cohesiveness. Their behaviour differed from the behaviour of their constituents. Overall, the mixtures with PPI differed from the remaining mixtures not only in their phase behaviour but also on the properties of their complexes. This deviation was attributed to weaker attractive forces between HMP and PPI. The results of the present study can be useful for the modulation of HMP based biopolymer complexes and their exploitation as structuring or encapsulating agents in food matrices.

1. Introduction

Carbohydrates and proteins are principal classes of biopolymers, widely exploited by the food industry as they share certain properties such as hydration and water binding, viscosity, gelation, emulsification and foaming ability (Goff & Guo, 2019). When these two types of biopolymers coexist in a solution, their interactions lead to one or two-phase systems due to three possible outcomes: miscibility, association or segregation (de Kruif & Tuinier, 2001; Syrbe, Bauer, & Klostermeyer, 1998). In miscibility, co-solubility exists and the biopolymers are spontaneously mixed and a one-phase system is formed. In segregation, the interaction between the unlike chains of proteins and polysaccharides are enthalpically unfavourable compared to those between like chains of each biopolymer (thermodynamic incompatibility). Thus, each biopolymer is surrounded by others of the same type (Gilsenan, Richardson, & Morris, 2003). This leads to mutual exclusionand the formation of two phases, each of which is rich in one biopolymer and has a small amount of the other. This phenomenon is called “phase separation” and occurs when one or both of the biopolymers have no charge or when both have a similar charge (Frith, 2010).

Enthalpically favourable interactions between the unlike chains of proteins and polysaccharides promote association between the two polymers. A typical case of these synergistic interactions is the electrostatic attraction between a polyanion and a polycation (Turgeon, Schmitt, & Sanchez, 2007) which at high concentrations can lead to either precipitation or coacervation (complex coacervation formation). This case can also be considered as phase separation as two phases are created, one being solvent rich and the other consisting of insoluble biopolymer complexes (Tolstoguzov, 2003). For low concentrations, soluble complexes are formed that are evenly distributed throughout the system.

The type of interactions in a protein – polysaccharide system is mainly determined by the type, concentration and characteristics (e.g., molecular weight, electrical charge, conformation) of the two biopolymers along with their mixing ratio, shear, pH, ionic strength and temperature (Matalanis, Lesmes, Decker, & McClements, 2010).

For a given protein – polysaccharide system the solution pH and the protein: pectin mixing ratio affect the intensity of the protein-polysaccharide interactions and the mechanism of complex formation between them, as they influence the number of charged reactive groups on the biopolymers surface, and the charge balance of biopolymers, respectively (Liu, Shim, Wang, & Reaney, 2015). The effect of pH on the

* Corresponding author.
E-mail addresses: ziogam19@gmail.com (M. Zioga), evageliou@aua.gr (V. Evageliou).

https://doi.org/10.1016/j.foodhyd.2023.108806
Received 19 November 2022; Received in revised form 18 April 2023; Accepted 20 April 2023
Available online 9 May 2023

interactions of a given protein–anionic polysaccharide mixture is studied by acidification of the mixture. At the higher end of the pH range, no significant interactions between the biopolymers take place as they both share similar charges. Further acidification of the mixture initiates the formation of soluble complexes. As the pH decreases, the protein surface becomes positively charged and thus, attracts the negatively charged polysaccharide molecules. These initial weak electrostatic interactions result in soluble complex formation (Lan, Ohm, Chen, & Rao, 2020; Zhang et al., 2018). As the pH continues to decrease, the primary soluble complexes aggregate to insoluble complexes. The insoluble complexes continue to grow in size and mass, with the phenomenon reaching its peak at a certain pH where the biopolymers are considered overall neutralized (Liu, Low, & Nickerson, 2009; Weinbreck, de Vries, Schrooyen, & de Kruif, 2003). At the same time, the solution remains homogeneous or changes from transparent to cloudy as a result from macroscopic phase separation (Liu et al., 2009). With further pH decrease the complexes start to dissociate and the mixture becomes transparent.

The usual way to monitor the interactions and complex formation between proteins and polysaccharides as a function of pH is by turbidity measurements, in which the absorbance of the mix solution at 600 nm is measured (Aryee & Nickerson, 2012). Turbidity measurements also provide information on mass or size and number of the insoluble protein-polysaccharide complexes (Liu et al., 2009; Ru, Wang, Lee, Ding, & Huang, 2012; Weinbreck et al., 2003; Yang, Anvari, Pan, & Chung, 2012). They are also a useful tool for evaluating the optimum conditions for complex coacervate formation as for a given mixture, critical pH values (namely pH_c, $pH_{\varphi 1}$, pH_{opt}, &$pH_{\varphi 2}$) can be designated from the changes in turbidity slope during titration from basic to acidic pH, in order to describe the steps of complex formation between proteins and negatively charged polysaccharides (Devi, Sarmah, Khatun, & Maji, 2017). pH_c is the pH corresponding to the first change in the slope. For pH values greater than pH_c, absorbance is low, resulting from the co-solubility of the two biopolymers. $pH_{\varphi 1}$ is the pH that a sharp increase in absorbance initiates indicating the formation of insoluble complexes. For pH values lower than $pH_{\varphi 1}$, the insoluble complexes continue to grow in size and mass and absorbance values further increase reaching a maximum value at pH_{opt}. Thus, pH_{opt} is the pH that charge neutrality is reached between the biopolymers and maximum coacervation is observed. As pH values are becoming more acidic than pH_{opt}, a decrease in absorbance is observed. Eventually, the absorbance values remain low and unchanged due to dissolution of the complexes. The pH that the plateau in absorbance is initiating is $pH_{\varphi 2}$ (Li, Zhang, Zhao, Ding, & Lin, 2018; Moschakis & Biliaderis, 2017).

Protein-polysaccharide interactions are utilized in the formation of many different colloidal structures such as particles, emulsions, gels, edible films and foams (Weiss, Salminen, Moll, & Schmitt, 2019). In recent years, protein-polysaccharide complex coacervation is considered a promising and efficient method of encapsulation of food ingredients as it is simple, scalable and reproducible, has low cost, and high encapsulation efficiency (up to 99%) (Timilsena, Akanbi, Khalid, Adhikari, & Barrow, 2019).

Pea Protein isolate (PPI) is a plant protein receiving a growing interest over the last years in food formulations due to its low cost and allergenicity, as well as its potential health benefits, which offer clean label to food products (Zha, Gao, Rao, & Chen, 2021). Furthermore, their larger molecular weight in comparison to animal proteins may result in a thicker shell for microencapsulation. PPI mainly consists of globulins and albumins (70–80% and 10–20% of PPI, respectively) (Zha, Dong, Rao, & Chen, 2019). Whey Protein isolate (WPI) and sodium caseinate (SC) are two widely used animal proteins. Whey proteins consists mainly of β-lactoglobulin, α-lactoalbumin and bovine serum albumin whereas sodium caseinate contains 4 types of phosphoproteins (a_{s1}, a_{s2},β-and κ-caseins). Among polysaccharides, pectin is a well-known polysaccharide for its interactions with proteins in order to improve the latter's functionality (Ru, Wang, Lee, Ding& Huang, 2012).

The objective of the current research was to gain insights in the effect of pH, mixing ratio and type of protein on the phase behaviour of concentrated protein – high methoxyl pectin systems and study the physicochemical, structural and mechanical properties of the insoluble complexes (coacervates) formed under the optimal coacervation conditions. We hypothesized that the differences in the origin (plant - animal) and the composition of each protein will affect the pectin-protein interactions and thus, the properties of the isolated complexes. Therefore, mixtures of HMP with either WPI, SC or PPI solutions were formed at pH 7 at protein: pectin mixing ratios ranging from 1:1 to 10:1. The pH was afterwards lowered to acidic conditions to promote complexation. The total biopolymer (HMP + protein) concentration ranged from 0.2 to 1.1%. Although several works on the interactions of HMP with the three proteins of the present studycan be found in literature (e.g. Raei, Rafe, & Shahidi, 2018; Ren et al., 2019; Shrestha, van't Hag, Haritos, & Dhital, 2023), to the best of our knowledge, no direct comparison of the three proteins on their complex coacervation with high methoxyl pectin under the same experimental conditions has been performed. Moreover, this comparison is performed at high total biopolymer concentrations. Despite the fact that the vast majority of the existing literature focuses on interactions at low total biopolymer concentrations (typically <0.3% wt) (Aryee & Nickerson, 2012; Rocha, Souza, Magalhaes, Andrade, & Goncalves, 2014), higher protein–polysaccharide concentrations are usually required for applications in encapsulation, fat-mimetics and texture modifiers (Klemmer, Waldner, Stone, Low, & Nickerson, 2012; Stenger, Zeeb, Hinrichs, & Weiss, 2017). The findings of the present study might be of interest for the incorporation of the formed complexes as structuring or encapsulating agents in food matrices.

2. Materials and methods

2.1. Materials & chemicals

High methoxyl pectin from apple (HMP, with 50–75% esterification; 93854), was obtained from Sigma-Aldrich (Steinheim, Germany). Its DE was determined by the titrimetric method proposed by Hosseini, Khodaiyan, and Yarmand (2016) as 56.5% whereas by FT-IR as 52%. Sodium caseinate (SC, Excellion® EM-7, 93% protein on dry basis), whey protein isolate (WPI, Lacprodan® DI-9224, 92% protein on dry basis) and yellow pea protein isolate (PPI, NUTRALYS® F85F, 84% protein on dry basis), were kindly donated by Alteco S.A. Food Ingredients (Athens, Greece), Arla Foods Ingredients Hellas (Athens, Greece) and Roquette (Lestrem, France), respectively. HCl and NaOH were from Sigma–Aldrich (Steinheim, Germany). Distilled water was used throughout.

2.2. Preparation and characterization of pectin – protein complexes

Protein (SC, WPI or PPI) stock solutions (5% wt) were prepared by dissolving the appropriate amount of protein in distilled water. After stirring for 4 h at room temperature, the protein solutions were stored at 4 °C overnight, for complete solubilisation. The PPI stock solution was filtered prior to use. Pectin stock solution (2% wt) was prepared by gradually adding pectin in deionized water at 90 °C, while stirring. The pectin solution was brought to correct weight by addition of water. When not in used, all solutions remained at 4 °C.

Protein – pectin mixtures were prepared based on the method proposed by Lan, Chen, and Rao (2018), by adding different amounts of protein stock solutions into the same amount of pectin stock solution to achieve protein:pectin ratios from 1:1 to 10:1 (1:1, 2:1, 4:1, 6:1, 8:1, 10:1). The final concentration of pectin was constant (0.1% wt) while the final concentration of each protein varied from 0.1% to 1.0 % wt (0.1, 0.2, 0.4, 0.6, 0.8, 1.0% wt). Solutions of each protein as well as pectin (0.1% wt) were also prepared and used as control.

The pH of each mixture was adjusted to 7 using 0.1M and 1M NaOH, added dropwise. Then, drops of HCl (0.1 and 1.0M) were added under magnetic stirring, gradually reducing the pH to 2 with a 1-unit

decrement. The use of various concentrations of HCl and NaOH was to minimize dilution effects and conductivity changes to mixture solutions. Acidification was performed after and not prior to mixing, as Bédié, Turgeon, and Makhlouf (2008) observed that in that case the size of complexes was constant and smaller.

Aliquots were taken every 1-unit change in pH for turbimetric and zeta potential measurements, and the construction of phase diagrams. For turbidity, absorbance of all samples was measured at 600 nm using a double-beam UV–Vis spectrophotometer (UV1800, Shimadzu Europa GmbH, Duisburg, Germany). The samples were contained within plastic cuvettes (path length of 1.0 cm) and distilled water was used as a blank reference. The surface charge of proteins, pectin, and their mixtures, reported as zeta-potential (mV) was determined with a Zetasizer Nano ZS90 instrument (Malvern Instruments Ltd., Worcestershire, UK). For the construction of phase diagrams, aliquots were left at room temperature overnight. After 24 h of standing, the phase diagrams were constructed based on visual observation. The state of each sample was classified into four groups, namely transparent/translucent solution, clear solution with precipitate, cloudy/milky solution and cloudy solution with precipitate.

2.3. Isolation and physicochemical, mechanical and structural properties of insoluble complexes

2.3.1. Isolation of insoluble complexes

Protein – pectin mixtures were prepared at the (selected from the experiments of §2.2) optimum conditions for insoluble complex formation and centrifuged at 4427×*g* for 10 min (Z 326 K, Hermle Labortechnik GmbH, Wehingen, Germany). The precipitates were collected, oven dried at 50 °C, and pulverized. The powders were stored in tightly closed containers in a dry and dark place. The coacervation yield was calculated based on Equation (1) (Yücetepe et al., 2021):

$$Yield\ (\%) = \frac{mass\ \ of\ dried\ complexes\ (g)}{total\ mass\ of\ pectin\ and\ protein\ in\ the\ formulation\ (g)} \times 100 \quad (1)$$

2.3.2. Physicochemical, mechanical and structural properties of individual biopolymers' and insoluble complexes' powders

2.3.2.1. Bulk, tapped and particle densityand porosity. The densities of the powders were measured based on the methods presented by Jinapong, Suphantharika, and Jamnong (2008), with modifications. Initially, powder (2 g) was gently introduced into a 10 mL dry graduated cylinder and levelled without compacting. The bulk density (ρ_{bulk}) of the powder was calculated as the ratio of weight to the untapped volume occupied in the cylinder (Equation (2)).

$$\rho_{bulk} = \frac{weight}{untapped\ volume} \quad (2)$$

The tapped density (ρ_{tapped}) was obtained by tapping the cylinder containing the powder, 100 times by hand, and calculated as the ratio of weight to the final tapped volume (Equation (3)).

$$\rho_{tapped} = \frac{weight}{tapped\ volume} \quad (3)$$

For the measurement of particle density ($\rho_{particle}$), 1 g of each powder was transferred into a 10 mL measuring cylinder with a glass stopper. Following the addition of 4 mL of petroleum ether, the cylinder was shaken until all the powder particles were suspended. A further 2 mL of petroleum ether (6 mL in total) was used to rinse down the particles on the wall of the cylinder. The total volume of petroleum ether with suspended powder was measured and used for the calculation of particle density as follows:

$$\rho_{particle} = \frac{weight\ of\ powder}{total\ volume\ of\ petroleum\ ether\ with\ suspended\ powder - 6} \quad (4)$$

Tapped (ρ_{tapped}) and particle ($\rho_{particle}$) densities were then used for the determination of porosity (ε) using the following equation:

$$\varepsilon = \frac{\rho_{particle} - \rho_{tapped}}{\rho_{particle}}_{\times 100} \quad (5)$$

All measurements were performed in triplicate.

2.3.2.2. Compressibility and cohesiveness. Carr Index (%)(CI) and Hausner ratio (HR) were calculated from bulk and tapped densities, in order to evaluate the compressibility/flowability and cohesiveness of the powders, respectively, using the following equations (Jinapong et al., 2008):

$$CI\ (\%) = \frac{\rho_{tapped} - \rho_{bulk}}{\rho_{tapped}} \times 100 \quad (6)$$

$$HR = \frac{\rho_{tapped}}{\rho_{bulk}} \quad (7)$$

2.3.2.3. Solubility. Solubility measurements were performed by the method of Ghasemi, Jafari, Assadpour, and Khomeiri (2017), with modifications. Powder (0.25 g) was added to distilled water (25 mL)and gently stirred for 1 h, at room temperature. Then, the dispersion was centrifuged at 4427×*g* for 5 min and the supernatant was collected, weighed, dried in an oven of 105 °C for 5 h and then, weighed again. Solubility (%) was determined based on the amount of powder dissolved in water. All measurements were done in triplicate.

2.3.2.4. Moisture content. Moisture was measured based on the method of Ghasemi et al. (2017), with modifications. Powder (0.10 g) was placed in an oven of 105 °C until constant weight, cooled and weighed. The moisture content was calculated using Equation (8), where $w_1$and $w_2$correspond to the initial and final weight of the sample after oven drying, respectively.

$$Moisture\ content\ (\%) = \frac{w_1 - w_2}{w_1} \times 100 \quad (8)$$

All measurements were done in triplicate.

2.3.2.5. Colour. For the evaluation of powder surface colour, a small amount of each powder was placed in a plastic cuvette and measured with aspectrocolorimeter (LC 100, Lovibond, Dortmund, Germany) using the CIE L*a*b* colour system. Three measurements per powder were conducted. Total colour difference (ΔE^*) and hue angle (h)were calculated by the following equations:

$$\Delta E^* = \sqrt{(\Delta L^*)^2 + (\Delta a^*)^2 + (\Delta b^*)^2} \quad (9)$$

$$h = \tan^{-1}\left(b*/a*\right) \quad (10)$$

For ΔE* the white tile of the colorimeter was used as the control.

2.3.2.6. pH, conductivity and kinematic viscosity. Solutions (1% wt) were prepared by adding the appropriate amount of powder to distilled water under gentle stirring for 1 h.Then, the pH of the solutions was measured with a pH meter (HI 2211, Hanna Instruments, RI, USA), the conductivity with a conductivity meter (SensoDirect Con 110, Lovibond, Dortmund, Germany) and the kinematic viscosity with a capillary viscometer (Ubbelohde) (diameter 1.36 mm, K = 0.3062 cSt/s; SUNLEX, Shanghai, China). All measurements were performed in triplicate.

2.3.2.7. Fourier transform infrared spectroscopy (FT-IR). An IROS-05

FTIR spectrophotometer (Ostec corporation group, Russia) equipped with a Mercury–Cadmium-Telluride (MCT) detector was used to obtain a total of three replicate spectra (three different sub-samples) from each powder (3 complexes, HMP, SC, WPI, PPI). A diamond crystal was employed for spectral recording from 400 to 4000 cm^{-1} at a resolution of 4 $cm^{-1}$and 32 scans. The speed of the interferometer moving mirror was 0.3164 mm/s. The diamond crystal provided a background spectrum, which was subtracted from each sample spectrum. Each spectrum was manipulated using the corresponding functions of the software (OMNIC ver. 8.2.0.387; Thermo Fisher Scientific Inc., Waltham, MA, USA) as follows: Each spectrum was "automatically smoothed", using the Savitzky–Golay algorithm (2nd order, 5-point window), baseline corrected using the "automatic baseline correction" (2nd order polynomial fit), averaged spectrum of each example triplet spectra was calculated, and the averaged spectra were normalized (absorbance from 0 to 1).

2.4. Statistical analysis

Analysis of variance (ANOVA) and least significant difference tests (LSD) were carried out on the data in order to determine significant differences among the samples. The significant level was $P < 0.05$ throughout the study. Analysis of data was carried out with statistical software package Statistica v.8.0 for Windows. Three experimental replications per powder were conducted.

3. Results & discussion

3.1. Effect of pH, protein-to-polysaccharide mixing ratio and type of protein on complex formation in protein – HMP mixtures

Initially, turbimetric measurements on HMP and the three proteins were performed. For HMP, its absorbance was negligible throughout the studied pH range (results omitted). This is indicative of HMP not forming aggregates that can scatter light. As HMP has a pKa ≈3.5, it is anionic over almost the entire pH range studied, leading to electrostatic repulsion between its molecules, which inhibits the contact of the molecules and the formation of agglomerates (Lan et al., 2018). Regarding the three proteins (Fig. 1), turbidity was low at both pH ends (2–3 and 6–7). For the intermediate pH values, absorbance increased up to a certain pH value, above which it decreased. This behaviour was also observed for other proteins solutions (Huang, Sun, Xiao, & Yang, 2012; Liu, Shim, Shen, Wang, & Reaney, 2017). It results from protein –protein aggregation, which reaches a maximum at its isoelectric point (pI) where lower solubility and neutral net charge is seen. Maximum absorbance for all three proteins was observed at pH ~4.5, in good agreement with the pI of 4.6 reported in literature for the three proteins (e.g. Burger & Zhang, 2019; Raei et al., 2018; Zhang & Zhong, 2013).

The turbimetric measurements for the mixtures, were reliable only for a limited number of samples. It is known that turbidity measurements cannot be applied to concentrated binary protein-polysaccharide systems as they present high initial turbidity which makes difficult for the subtle absorbance changes upon the formation of soluble complexes to be recorded by the spectrophotometer. The higher mixing ratios of the present work resulted in concentrated systems with absorbance values higher than 1 and as such they were not taken under consideration. For the lower mixing ratios (results not shown), a typical turbimetric curve was reported and all four critical boundary pH values (pH_c, $pH_{\varphi1}$, pH_{opt}, $pH_{\varphi2}$) were identified as well as the corresponding four different phase behaviours (i.e., for pH values greater than pH_c, co-solubility; for pH values in the range of pH_c - $pH_{\varphi1}$: formation of soluble complexes; for pH values in the range of $pH_{\varphi1}$ - $pH_{\varphi2}$: formation of complex coacervates and for pH values lower than $pH_{\varphi2}$: dissolution of complexes) (Li et al., 2018; Moschakis & Biliaderis, 2017). Moreover, absorbance increased with protein content. Thus, the protein: pectin mixing ratio was very important for turbidity as a greater amount of protein molecules were available per pectin chain for complexation (Ru et al., 2012). This phenomenon was also affected by the type of the protein as the same mixing ratio resulted in different absorbance values for the three proteins, thus, different extent of intermolecular associations.

In order to overcome the limitations of turbidity measurements for the mixtures of the present work, and thus, to be able to study the protein-pectin interactions for all the selected ratios and pH values, a phase diagram per protein was constructed. The phase diagram is a good way to present the phase behaviour of concentrated protein-polysaccharide mixtures and detect the boundary pH range of their co-solubility, soluble and insoluble complexes' formation (Dai, Jiang, Shah, & Corke, 2017). Fig. 2a-c presents the corresponding phase diagrams for all the mixtures of the present study constructed following their visual observation after standing at room temperature for 24 h. As already mentioned in the Introduction, complex formation during acidification has an impact on the appearance of the mixtures. Thus, Fig. 2d-f shows the appearance of the mixtures for all proteins, mixing ratios and pH values. Each phase diagram illustrates 4 distinguishable phase behaviours: transparent/translucent solution (o), clear solution with precipitate (●), cloudy/milky solution (Δ) and cloudy solution with precipitate (▲). For comparison reasons, the changes of the protein solutions as a function of pH is also included. However, the corresponding data for the pectin solution is not presented as the solution was translucent across the entire pH range studied. As expected, pH, mixing ratio and type of protein were important for our observations. Co-solubility, soluble complex and insoluble complex formation areas

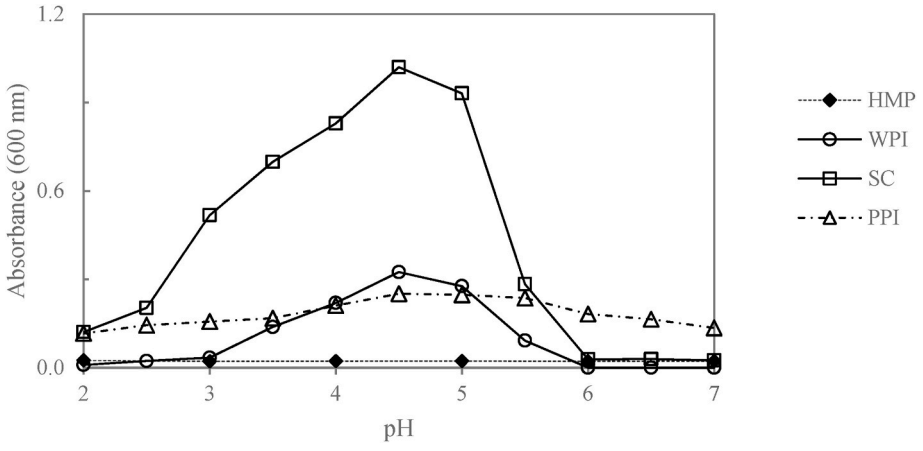

Fig. 1. Turbidity curves of WPI, SC, PPI and HMP at a concentration of 0.1% wt, during acid titration from pH 7 to 2 [Sodium caseinate (SC), Whey protein isolate (WPI), pea protein isolate (PPI), High methoxyl pectin (HMP)].

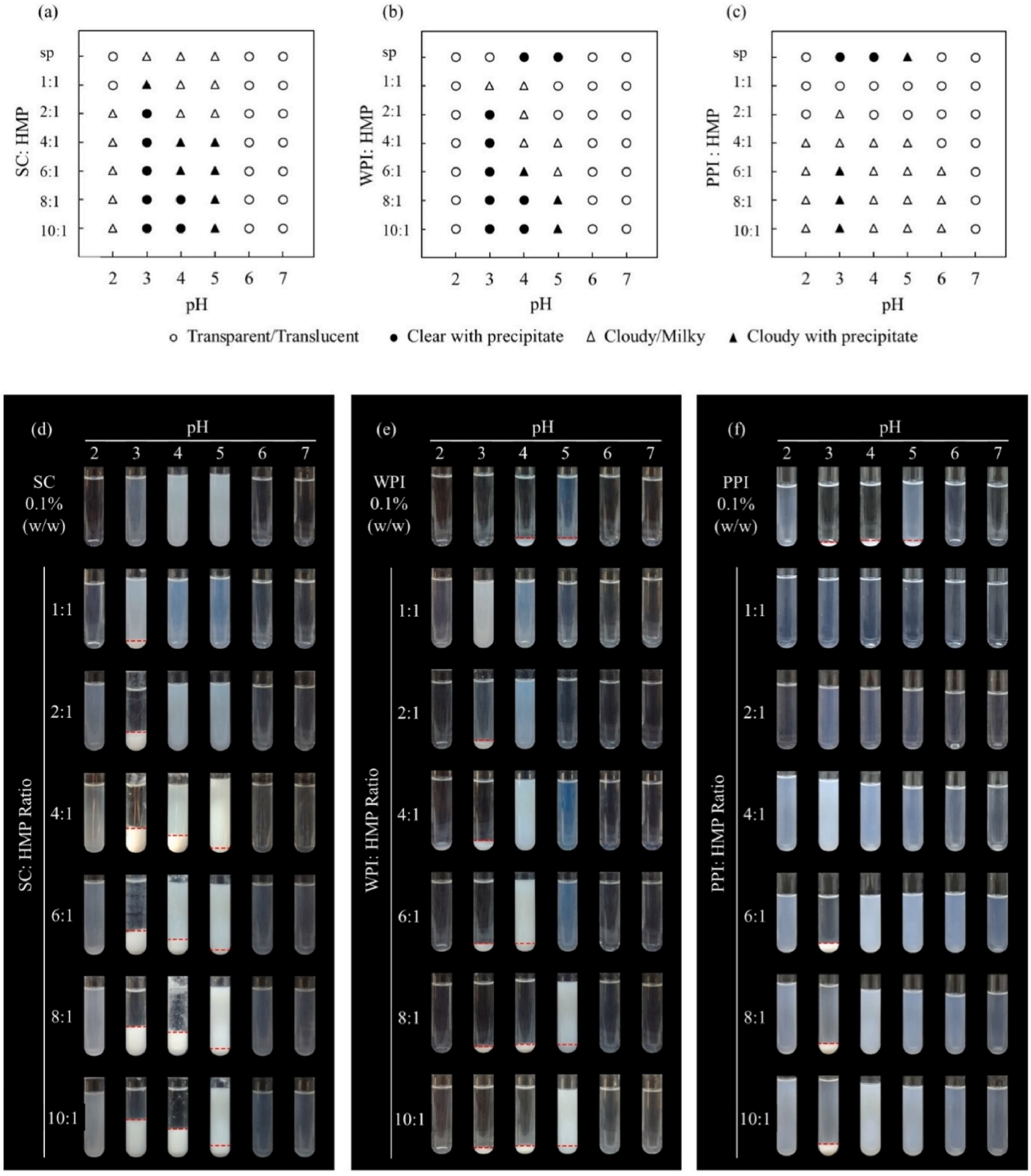

Fig. 2. (a–c) Phase diagrams of protein (SC, WPI or PPI)-HM pectin mixtures and single protein (sp, 0.1% wt) during acid titration from pH 7–2. (d–f) The depiction of phase diagrams includes transparent/translucent solutions (o), clear solutions with precipitate (●), milky/cloudy solutions (Δ) and cloudy solutions with precipitate (▲)[Sodium caseinate (SC), Whey protein isolate (WPI), pea protein isolate (PPI), High methoxyl pectin (HMP)].

were seen in all diagrams.

The observation of soluble complexes, represented as turbid and milky solutions without precipitation (Δ), depended on the protein. For example, SC-HMP soluble complexes (Fig. 2a) were seen for pH values 4–5 for the mixing ratios of 1:1 and 2:1 and pH 2 for all mixing ratios apart from 1:1. In the case of WPI-HMP, soluble complex formation was limited and mainly seen at ratios 1:1 (pH values 3 & 4), 2:1 (pH 3), 4:1 (pH values 4 & 5) and 6:1 (pH 5). PPI-HMPsoluble complexes were observed for all ratios apart from 1:1, with greater pH range reported for ratios 4:1 to 10:1. As reported earlier, soluble complex formation is

indicative of weak electrostatic interactions between pectin and the three proteins.

Regarding insoluble complexes, their formation was observed with two different phase behaviours (▲, ●) and it depended on the protein. For SC-HMP mixtures, insoluble complexes were formed at pH 3 (all ratios) and pH values 4 & 5 (ratios 4:1 to 10:1). WPI-HMP mixtures showed insoluble complex formation at pH 3 (ratios 2:1 to 10:1), pH 4 (ratios 6:1 to 10:1) and pH 5 (ratios 8:1 & 10:1). For PPI-HMP mixtures, the formation of insoluble complexes was limited to pH 3 and just for the ratios 6:1 to 10:1.

For pH 7, the mixtures with HMP of all three proteins were translucent [represented as (o)] for all mixing ratios, indicating protein – pectin co-solubility (Liu et al., 2015; Zhang et al., 2018). Co-solubility is also seen for other pH values, but its extent depended on the protein. SC-HMP mixtures were translucent at pH 2 (ratio 1:1) and pH 6 (all ratios) whereas WPI-HMP mixtures were translucent at pH values 2 and 6 for all ratios. PPI-HMP mixtures with 1:1 ratio exhibited co-solubility throughout the pH range whereas those with 2:1 ratio showed

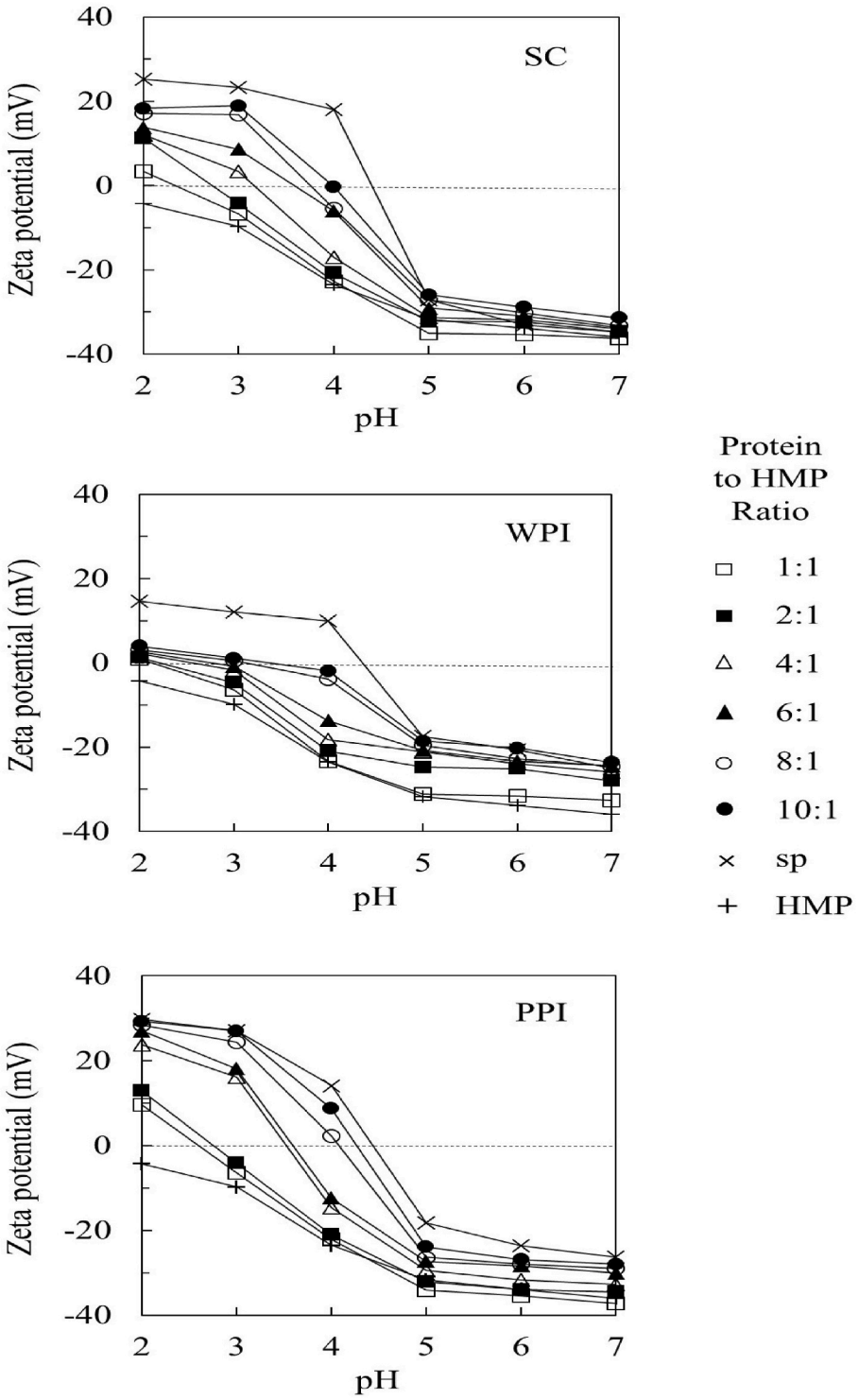

Fig. 3. pH dependence of zeta potential (mV) of protein (SC, WPI or PPI)- HM Pectin mixtures, as well as pectin (HMP) and the proteins (sp) on their own (0.1% wt) during acid titration from pH 7–2 [Sodium caseinate (SC), Whey protein isolate (WPI), pea protein isolate (PPI), High methoxyl pectin (HMP)].

co-solubility for all pH values apart from pH 3. For all mixtures, the lower ratios presented a greater one phase region compared to the higher ones, which was more evident for PPI-HMP mixtures. Thus, the higher protein concentration favoured the formation of insoluble rather than soluble complexes as more protein-protein aggregates are available for complexation with pectin (Pillai et al., 2019). Moreover, the aggregation of all protein particles also increased steadily as the pH decreased, especially at pH values close to their pI (Lan et al., 2018).

Since the formation of insoluble or soluble protein-polysaccharide complexes mostly results from the electrostatic attractions between the two biopolymers (Yang et al., 2012), zeta potential values of the mixtures as a function of ratio and pH were measured and presented in Fig. 3. The corresponding curves of pectin and protein solutions are also presented. Regarding HMP, the zeta potential values of its solution, were negative across the whole pH range (−36.0 to −4.3 mV), as expected since pectin is an anionic heteropolysaccharide (Nep & Conway, 2011). The zeta potential values of the protein solutions were greatly affected by pH as they increased with decreasing pH. They started with a negative charge at pH 7 (−34.8 mV, −25.0 mV and −26.4 mV for SC, WPI and PPI solutions, respectively), which eventually became positive at pH 2 (25.2 mV, 14.5 mV and 29.7 mV for SC, WPI and PPI solutions, respectively) after crossing over the zero charge point near their isoelectric point (pH~ 4.5). The lower zeta potential absolute value of HMP at pH 2 compared to the proteins can explain the observed co-solubility following the vanishing of the formerly formed insoluble complexes (Fig. 2) (Lan et al., 2020).

Zeta potential values for all mixtures, were in-between the values measured for pectin and the corresponding protein. Furthermore, for all of them, values increased as the pH decreased in the same trend as for the proteins. For all pH values, zeta potential values increased with increased mixing ratio (Fig. 3). As the zeta potential value of the mixtures represents the zeta potential values of the biopolymer complexes as well as of the non-interacting individual biopolymers, this shifting can result from the higher zeta potential of the protein compared to the polysaccharide (Duhoranimana et al., 2018; Liu et al., 2015). With increasing mixing ratio more protein molecules are available in the mixture to achieve electro-neutrality of the insoluble complex. Thus, the protein has a smaller positive charge at higher pH and higher mixing ratio (Yang et al., 2012).

For the elucidation of the type (attractive or repulsive) and the magnitude of the interactions as a function of pH, the strength of electrostatic interaction (SEI) of protein–pectin was calculated as the multiplication of zeta potential values of individual biopolymer at each pH (e.g. Timilsena, Wang, Adhikari, & Adhikari, 2016). For example if for a given pH the zeta potential for pectin and protein is X and Y, respectively, the SEI is given by (X*Y). The calculated SEI values of all mixtures are presented in Fig. 4a. Negative SEI values indicate attractive forces between biopolymer molecules. Moreover, the pH range that SEI gets its higher values is where the attraction between opposite biopolymers is the stronger (Espinosa-Andrews et al., 2013). As seen from Fig. 4a, attractive forces for the mixtures appeared at a pH range of 2.5–4.5 for both WPI-HMP and SC-HMP mixtures and 4–7 for the PPI-HMP mixture, with their greater values seen between 3-4 and 4–5, respectively. Clearly, the SC-HMP mixture had the stronger attraction between its constituent biopolymers of all complexes, with the PPI-HMP mixture showing very low attraction between PPI and HMP. The lower protein concentration (84%) in PPI compared to the other two proteins contributes to the observed behaviour of PPI-HMPmixtures.

Regarding the boundary pH values, in cases with concentrated binary systems such as ours, that phase diagrams are used for describing their phase behaviour, the only boundary pH values that can be determined are $pH_{\varphi 1}$ and $pH_{\varphi 2}$. In the present work, they could be determined as the pH values at which a phase transits from ▲ to ●. However, pH_{opt} cannot be determined by a phase diagram, but, a good alternative is its estimation from the zeta potential curves as the pH that net charge neutrality (zero zeta potential value) is achieved, which is usually

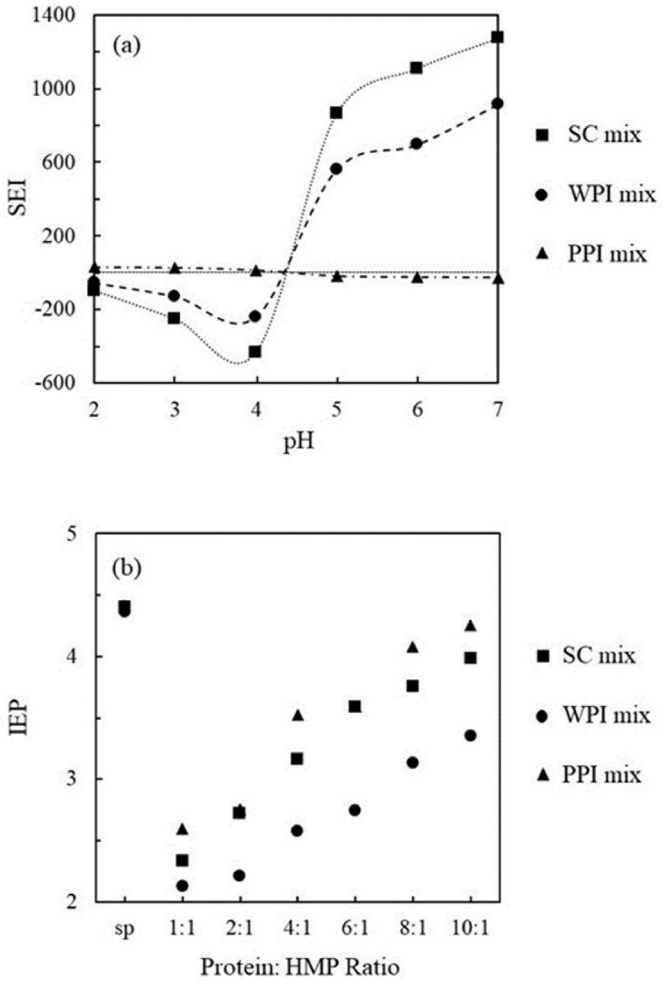

Fig. 4. (a) SEI of protein-HMP mixtures and (b) IEP of all protein-HMP mixtures as well as the pI of the individual proteins (sp) [Sodium caseinate (SC), Whey protein isolate (WPI), pea protein isolate (PPI), High methoxyl pectin (HMP)].

regarded as an isoelectric point (IEP) (Anema & de Kruif, 2014). According to literature (e.g. Plati, Ritzoulis, Pavlidou, & Paraskevopoulou, 2021), the most extensive protein – polysaccharide interactions occur at the point where the electrical charge of biopolymer mixtures is neutral. The IEP for the mixtures and the proteins of the present study was determined (Fig. 4b). As seen from Fig. 4b, IEP moved to more acidic pH values as the ratio decreased and it was in the area of 2.5–4.5. Over this range, pectin and proteins are oppositely charged (Fig. 3) and thus, strong electrostatic interactions between the negatively charged carboxyl groups of the pectin molecules and the positively charged amino groups of the protein molecules are occurring resulting in complex formation.

3.2. Physicochemical, mechanical and structural properties of protein-pectin complexes

The physicochemical, mechanical and structural properties of selected protein – pectin mixtures were studied then. Based on our finding (§3.1) complexes were formed at protein: pectin mixing ratio 6:1, and at pH 4 for SC and WPI or pH 3 for PPI. The complex coacervation yield was 91.6, 51.4 and 7.6% forSC–HMP, WPI-HMP and PPI–HMP complexes, respectively. Given the fact that all complexes had the same biopolymer concentration, this finding is related to the strength of the electrostatic interactions indicating stronger and weaker interactions for SC–HMP and PPI–HMP complexes, respectively.

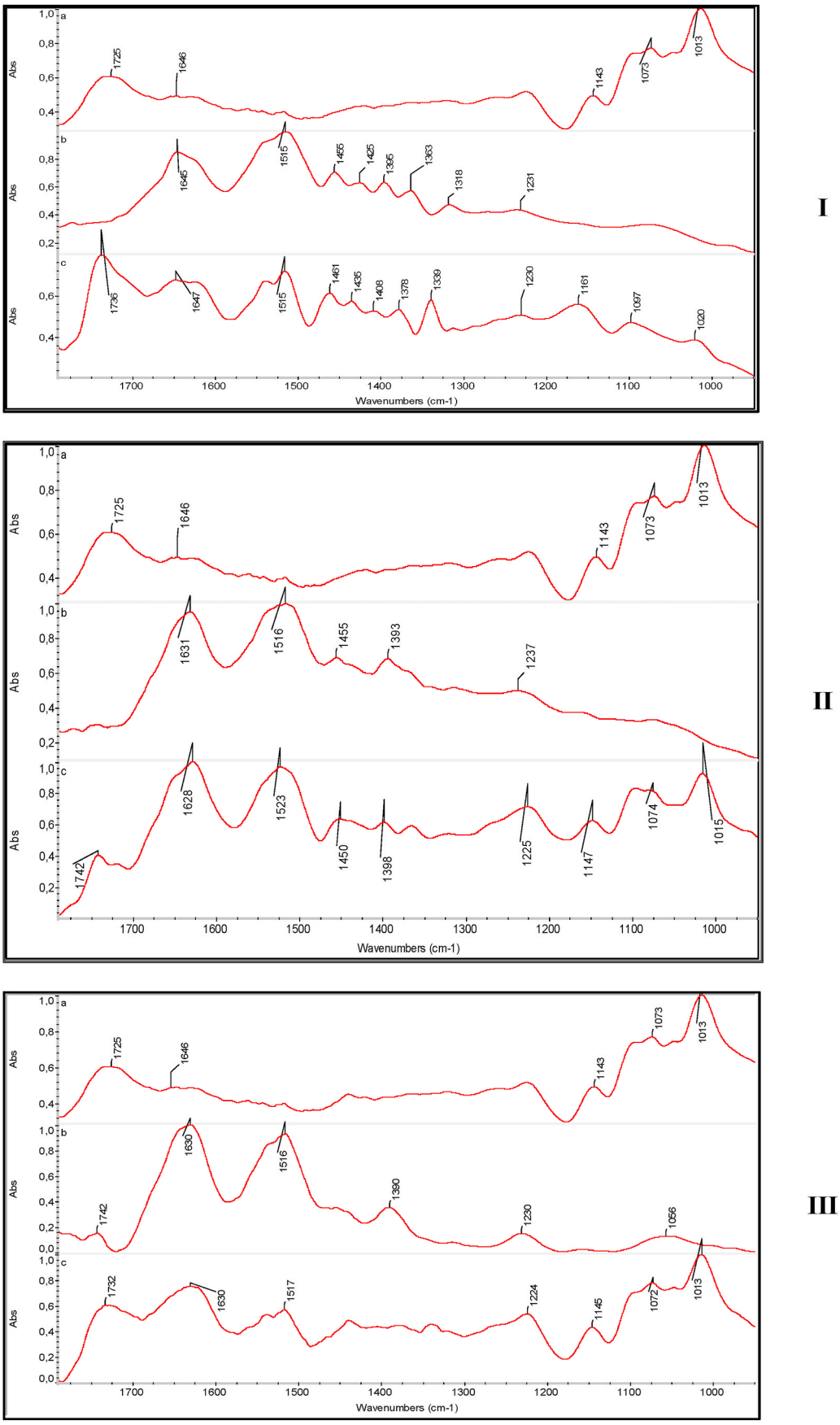

Fig. 5. The spectral region 1790-950 cm^{-1} of: I. a) High methoxyl pectin (HMP), b) Sodium caseinate (SC), c) HMP-SC complex; II. a) High methoxyl pectin (HMP), b) Whey protein isolate (WPI), c) HMP-WPI complex; III. a) High methoxyl pectin (HMP), b) Pea protein isolate (PPI), c) HMP-PPI complex.

The isolated complexes in the form of a powder were then studied in terms of several physicochemical, mechanical and structural properties. These properties are defining the characteristics and the behaviour of the powders during processing, handling and storage (Jaya & Das, 2004; Seerangurayar, Manickavasagan, Al-Ismaili, & Al-Mulla, 2017). For comparison reasons HMP and the three proteins powders were also studied.

The first property studied was colour (Table 1), the importance of which relates to the fact that it determines the macroscopic aspect of the products that the powder is incorporated as an ingredient (Bordón et al., 2021). Regarding their lightness, [L*] varied from ~50 to ~90. All proteins ([L*]: ~79–91) were brighter than pectin ([L*]~70). SC and WPI shared statistically the same lightness which was higher than that of PPI. The presence of pectin affected the lightness of the mixtures as they all presented [L*] values lower than those of the proteins. Among them, the WPI-HMP complex was the brighter ([L*] ~73) followed by the SC-HMP one ([L*]~69). Values of [a*] were positive for all the mixtures ([a*]: ~7-~15), pectin ([a*] ~9] and PPI ([a*] ~7). The remaining proteins had [a*] values close to zero. Positive [b*] values were reported for all powders. PPI showed greater [b*] (~22) values than the other two proteins (~9) and slightly greater than pectin (~20). The mixtures also presented high [b*] values ranging from 20 to 25. PPI-HMP exhibited the greater value and WPI-HMP the lower. Moreover, SC and WPI powders had the lower colour difference and greater hue of all studied powders. On the other edge, the PPI-HMP powder had the greater colour difference and lower hue value. Overall, the presence of pectin seems to be a critical parameter for colour.

The next parameters evaluated were solubility and moisture content. Table 2 presents the corresponding values. Once again, the behaviour of the mixtures differed significantly from the individual biopolymers. Biopolymers had higher solubility and lower moisture content than the mixtures. All measured moisture content values were within or close to the range of 1–5% that is generally accepted for food powders (Opaliński, Chutkowski, & Hassanpour, 2016). HMP and SC showed the lower moisture content (~3.4%), followed by PPI (~4%) and WPI (~6%). Mixtures had a moisture content of ~5.3, 6.2 and 7% for PPI-HMP, WPI-HMP and SC-HMP mixtures, respectively. Our findings on the mixtures can be attributed to the strength of each complex. As already mentioned, electrostatic interactions and bonds were stronger for the SC–HMP complex and weaker for the PPI–HMP complex, thus, leading to strong and weak complexes, respectively. In strong complexes, water binding within the complex increases and thus, water's movement is prevented. In a weak complex, water is more easily removed during drying (Ghasemi et al., 2017). Regarding solubility, HMP, SC and WPI exhibited solubility greater than 90% whereas PPI had a solubility of ~27%. The solubility of the mixtures ranged from 1.76 to ~6.2%, with the PPI-HMP mixture being the more soluble. The difficulty in breaking these bonds for dissolving the complex powder in water is probably greater for the stronger SC–HMP complex which leads to lower solubility. At the same time, in stronger complexes, bigger particles are formed which need more time to dissolve in water (Ghasemi et al., 2017).

Table 1
Colour parameters (L*, a*, b*), ΔE* and hue (h) of HMP, SC, WPI, PPI powders as well as the corresponding insoluble complexes' powder (SC or WPI or PPI and HMP). [Sodium caseinate (SC), Whey protein isolate (WPI), pea protein isolate (PPI), High methoxyl pectin (HMP)].

Sample (powder)	[L*]	[a*]	[b*]	[ΔE*]	h
HMP	$69.83^{a} \pm 0.41$	$9.13^{a} \pm 0.29$	$20.17^{a} \pm 0.26$	$33.53^{a} \pm 0.64$	$65.64^{a} \pm 0.62$
SC	$89.90^{b} \pm 1.49$	$-0.43^{b} \pm 0.12$	$9.50^{b} \pm 0.08$	$9.55^{b} \pm 1.34$	$92.62^{b} \pm 0.95$
WPI	$91.30^{b} \pm 0.75$	$0.43^{c} \pm 0.24$	$8.40^{c} \pm 0.22$	$7.82^{c} \pm 0.83$	$87.03^{c} \pm 1.99$
PPI	$79.13^{c} \pm 0.05$	$6.77^{d} \pm 0.12$	$21.70^{d} \pm 0.16$	$26.81^{d} \pm 0.22$	$72.68^{d} \pm 0.22$
SC-HMP	$68.97^{a} \pm 0.52$	$7.47^{e} \pm 0.41$	$21.90^{d} \pm 0.29$	$34.69^{a} \pm 0.80$	$71.18^{d,e} \pm 1.03$
WPI-HMP	$73.27^{d} \pm 0.87$	$7.20^{de} \pm 0.08$	$20.40^{a} \pm 0.37$	$30.38^{e} \pm 1.10$	$70.56^{e} \pm 0.30$
PPI-HMP	$49.53^{e} \pm 1.02$	$14.73^{f} \pm 0.41$	$24.53^{e} \pm 0.78$	$54.31^{f} \pm 0.58$	$59.01^{f} \pm 0.17$

(*) Values with different superscripts for each property are significantly different ($p < 0.05$).

Table 2
Solubility, moisture content, pH, conductivity and kinematic viscosity of HMP, SC, WPI, PPI powders as well as the corresponding insoluble complexes' powder (SC or WPI or PPI and HMP) [Sodium caseinate (SC), Whey protein isolate (WPI), pea protein isolate (PPI), High methoxyl pectin (HMP)].

Sample (powder)	Solubility (%)	Moisture content (%)	pH of 1% wt solution	Conductivity (mS/cm) Of 1% wt solution	Kinematic viscosity (cSt) of 1% wt solution
HMP	$90.96^{a} \pm 0.64$	$3.09^{a} \pm 0.18$	$2.71^{a} \pm 0.02$	$0.54^{a} \pm 0.00$	$3.86^{a} \pm 0.02$
SC	$93.36^{b} \pm 1.00$	$3.45^{a} \pm 0.07$	$6.90^{b} \pm 0.04$	$0.27^{b} \pm 0.01$	$1.58^{b} \pm 0.01$
WPI	$92.10^{ab} \pm 1.31$	$4,91^{b} \pm 0.13$	$6.83^{b} \pm 0.04$	$0.30^{c} \pm 0.01$	$1.43^{c} \pm 0.01$
PPI	$27.36^{c} \pm 0.80$	$4.05^{c} \pm 0.18$	$7.94^{c} \pm 0.04$	$0.27^{b} \pm 0.00$	$1.47^{d} \pm 0.01$
SC-HMP	$1.76^{d} \pm 0.07$	$6.96^{d} \pm 0.10$	$3.85^{d} \pm 0.05$	$0.06^{d} \pm 0.01$	$1.39^{e} \pm 0.00$
WPI-HMP	$2.42^{d} \pm 0.02$	$6.23^{e} \pm 0.17$	$4.22^{e} \pm 0.04$	$0.02^{e} \pm 0.00$	$1.39^{e} \pm 0.01$
PPI-HMP	$6.19^{e} \pm 0.17$	$5.28^{b} \pm 0.27$	$3.40^{f} \pm 0.02$	$0.13^{f} \pm 0.01$	$1.45^{cd} \pm 0.01$

*: Values with different superscripts for each property are significantly different ($p < 0.05$).

The next evaluated parameter was conductivity which expresses the easiness of a solution in electric current transfer. The higher the concentration of ions present in a solution, the higher the conductivity. According to our measurements, pectin had the highest conductivity (0.5 mS/cm) followed by the proteins (0.27–0.3 mS/cm), while the complexes showed much lower conductivity values (0.02–0.1 mS/cm); thus, significantly lower ion concentration in their solutions. This results from obtaining the complexes under electrical neutrality conditions, as described earlier, and is in good agreement with the decreased solubility observed for the complex powders (Table 2).

The pH of 1% (wt) aqueous solutions of all powders was measured and its values are presented in Table 2. According to our measurements, pectin had the more acidic pH (~3) whereas the proteins' pH was close to 7. The pH of the mixtures ranged from ~3.5 to 4.2. The kinematic viscosity of all aqueous powder solutions was also measured, at room temperature. Its values (Table 2) were affected by the measured material as well as their pH. The acidic pectin solution had the greater kinematic viscosity (~3.9 cSt) probably due to interactions between the pectin chains. Guimarães, Coelho Júnior, and Garcia Rojas (2009) reported greater viscosity values of aqueous pectin solutions of acidic pH compared to other pH values, and attributed this observation to the increased hydrophobic interactions of the methyl ester groups (-$COOCH_3$). The viscosity of the protein solutions ranged from ~1.4 to 1.6 cSt. Given that the pH of these solutions was close to 7, thus, greater than their pI, their molecules have a negative overall charge. As a result, the protein molecules repel each other, with that electrostatic repulsion suppressing their mobility and leading to an increase in the solution viscosity (Hong, Iwashita, & Shiraki, 2018). As expected, due to the thickening properties of proteins and polysaccharides, all the solutions of the individual biopolymers had greater viscosity than pure water (1.37 cSt ± 0.01). Mixtures showed viscosity values from 1.39 to 1.45 cSt. With the exception of the PPI-HMP mixture, the mixtures had lower kinematic viscosity than their constituents and exhibited values very

close to that of water. Thus, their thickening ability was reduced compared to the individual biopolymers. Their low conductivity and reduced solubility might explain this finding.

Other useful indicators of the powder's behaviour are bulk, tapped and particle densities. The first two densities are used for the calculation of Carr index (CI) and Hausner ratio (HR), which are generally employed for the determination of the powder's flowability (Seerangurayar et al., 2017). Tapped and particle densities are used for the calculation of porosity. The measured densities, CI, HR and porosity values for all powders are presented in Table 3. Bulk density varied from 0.3 to 0.48 g/cm^3 whereas tapped density from 0.36 to 0.73 g/cm^3. For the individual biopolymers, HMP had the greater values for both densities, followed by PPI, SC and WPI. Among the mixtures, the SC-HMP mixture had the greater bulk density whereas the WPI-HMP mixture had the greater tapped density. In all cases, tapped density was higher than bulk density as tapping results in a more dense packing because the smaller particles occupy the voids between the larger particles (Hernández--Nava, López-Malo, Palou, Ramírez-Corona, & Jiménez-Munguía, 2020).

Carr Index (CI) and Hausner ratio (HR), which correlate to the powder's flowability and cohesiveness, respectively, were calculated then and their values are also shown in Table 3. Powder flowability is described as very good (CI: <15%), good (CI: 15–20%), fair (CI: 20–35%), bad (CI: 35–45%) or very bad (CI: >45%). Regarding powder cohesiveness, it is described as high (HR > 1.4), intermediate (HR: 1.2–1.4) and low (HR < 1.2) (Jinapong et al., 2008). WPI, with a CI of ~16% has a better flowability than SC (~25%) and HMP and PPI (both ~30%). Thus, apart from WPI, which has a good flowability, the remaining biopolymers show fair flowability. Regarding the mixtures, WPI-HMP and PPI-HMP mixtures had the same CI (~35%) whereas SC-HMP had a CI of ~28%. Thus, all mixtures did not have a good flowability. For the biopolymers, their HR values ranged from 1.19 to 1.4, showing moderate cohesiveness, whereas for the mixtures the HR values ranged from 1.39 to 1.56, thus, showing high cohesiveness.

Particle density for individual biopolymers ranged from ~1–2.36 g/cm^3. HMP exhibited the higher value followed by SC and WPI with PPI (both ~1 g/cm^3). WPI-HMP and PPI-HMP mixtures shared statistically the same particle density (~1.16) which was lower than that of the SC-HMP mixture. More or less, the same trend was observed for porosity. Porosity values for individual biopolymers ranged from ~39 to ~73%, with HMP and PPI exhibiting the higher and lower values, respectively. The SC-HMP mixture had the greatest porosity (~54.5%) followed by PPI-HMP and WPI-HMP mixtures (~40 and 38%, respectively).

Overall, the mixtures showed bad flowability and high cohesiveness whereas the biopolymers fair flowability and moderate cohesiveness. Moreover, the mixtures had greater bulk and tapped densities and lower porosity compared to the individual biopolymers. Generally, all of the above parameters are affected by the particle size and its distribution, as well as the moisture content of the powder (Jaya & Das, 2004; Seerangurayar et al., 2017). Thus, the observed behaviour of the mixtures in comparison to the individual biopolymers may result from a smaller particle size, as in that case the void between the particles is smaller and thus, the particles' packing is denser (Seerangurayar et al., 2017). As a result, higher tapped densities but lower porosities can be observed. Moreover, the contact surface between the particles is greater, resulting in stronger interparticle forces, and stronger flow resistance (Fitzpatrick, Iqbal, Delaney, Twomey, & Keogh, 2005). Regarding moisture content, the increased weight of the powders due to the presence of water may also result in greater density values (Chegini & Ghobadian, 2005). As already reported, the mixtures had greater moisture contents than the biopolymers on their own.

Finally, in order to investigate the structure of the biopolymers and their complexes, FT-IR analysis was performed. As the main differences were found in the spectral region 1790-950 cm^{-1}, Fig. 5 presents this spectral region of the FTIR spectra of all powders. For better understanding of the possible pectin-protein interactions, Fig. 5I presents the spectra of HMP, SC and their complex, Fig. 5(II) presents the spectra of HMP, WPI and their complex and Fig. 5(III) presents the spectra of HMP, PPI and their complex.

Regarding HMP [Fig. 5 (Ia, IIa, IIIa)], which participates in all three complexes, the main peaks were seen at 1725, 1646, 1143, 1073 and 1013 cm$^{-1.}$ The first two peaks represent the stretching vibration of the carbonyl group (>C═O) in the esterified carboxyl group and the carboxylate group, respectively. The latter three peaks indicate C–O–C stretching (stretching of glycosidic bond, ring), a combination of C–O (stretching) and –OH in-plane bending and C–C and C–O stretching, respectively (Synytsya, Čopíková, Matějka, & Machovič, 2003). For SC (Fig. 5-Ib) the peak at 1645 cm^{-1} was attributed to > C═O stretching vibration (amide I) whereas that in 1515 cm^{-1}was assigned to N–H bending vibration with contribution of C–N stretching vibrations (amide II) (Ren et al., 2019). The peaks at 1455, 1425 and 1396 cm^{-1} were ascribed to C–H bending deformation vibration, –CH_2- bending vibration and CH_3 symmetrical deformation, respectively (Ren et al., 2019; Socrates, 2004). Finally, the peaks at 1363, 1318 and 1231 cm^{-1}were associated to P═O (symmetric stretching), amide III and β-sheet vibrations, respectively (Socrates, 2004). In the case of the SC-HMP complex (Fig. 5-Ic) noticeable shifts of the peaks in the spectral region 1460–950 (except for the peak at 1230 cm^1) were observed.

Fig. 5-II compares the spectra of HMP, WPI and their complex. For WPI (Fig. 5-Ib) the peaks at 1631 and 1516 cm^{-1}were attributed to > C═O stretching vibration (amide I) and the N–H bending vibration with contribution of C–N stretching vibrations (amide II), respectively (Raei et al., 2018). The peaks at 1455, 1393 and 1237 cm^{-1} were associated to C–H bending deformation vibration, CH_3 symmetrical deformation and β-sheet vibrations, respectively (Raei et al., 2018; Socrates, 2004). When looking at the spectrum of the WPI-HMP complex, a noticeable shift of the peak at 1237 cm^{-1} (to 1225 cm^{-1}) of the WPI spectrum is observed. Moreover, the 1725 cm^{-1} peak of the HMP spectrum, appears in the complex spectrum at 1745 cm^{-1} while that at 1013 cm^{-1} was decreased.

Regarding the last combination (HMP and PPI), Fig. 5-III shows the relevant spectra. The PPI spectrum (Fig. 5-IIIb) reveals peaks at 1631 and 1516 cm^{-1}, which were assigned to > C═O stretching vibration (amide I) and the N–H bending vibration with contribution of C–N stretching vibrations (amide II), respectively (Shrestha et al., 2023). The peak observed at 1742 cm^{-1} associates with ester functional groups. Literature reports this peak for pea and chickpea protein isolates and attributes it to the presence of lipids (Ricci et al., 2018). The remaining

Table 3
Bulk, tapped and particle densities, porosity, Carr Index (CI) and Hausner ratio (HR) of HMP, SC, WPI, PPI powders as well as the corresponding insoluble complexes' powder (SC or WPI or PPI and HMP) [Sodium caseinate (SC), Whey protein isolate (WPI), pea protein isolate (PPI), High methoxyl pectin (HMP)].

Sample (powder)	Bulk density (g/cm^3)	Tapped density (g/cm^3)	Particle density (g/cm^3)	Porosity (%)	Carr Index (CI)(%)	Hausner ratio (HR)
HMP	0.45^a ± 0.00	0.65^a ± 0.00	2.36^a ± 0.14	72.69^a ± 0.00	30.07^a ± 0.74	1.43^a ± 0.02
SC	0.36^b ± 0.00	0.48^b ± 0.01	1.25^{be} ± 0.00	61.60^b ± 0.44	25.15^b ± 0.21	1.34^b ± 0.00
WPI	0.30^c ± 0.00	0.36^c ± 0.00	0.92^c ± 0.08	60.57^c ± 0.33	15.73^c ± 0.67	1.19^c ± 0.01
PPI	0.43^d ± 0.00	0.61^d ± 0.00	1.00^{cd} ± 0.00	39.39^d ± 0.00	29.28^{ad} ± 0.72	1.41^{ad} ± 0.01
SC-HMP	0.48^e ± 0.01	0.67^e ± 0.00	1.46^b ± 0.04	54.47^e ± 0.00	27.99^d ± 0.82	1.39^d ± 0.02
WPI-HMP	0.47^f ± 0.01	0.73^f ± 0.01	1.18^{de} ± 0.07	38.00^f ± 1.06	35.94^e ± 0.96	1.56^e ± 0.02
PPI-HMP	0.45^a ± 0.00	0.69^g ± 0.00	1.14^{cde} ± 0.03	39.70^d ± 0.00	34.58^e ± 0.69	1.53^f ± 0.02

*: Values with different superscripts for each property are significantly different ($p < 0.05$).

peaks at 1390, 1230 and 1056 cm^{-1}were associated to CH_3 symmetrical deformation, β-sheet vibrations and C–O–C stretching, respectively (Shrestha et al., 2023; Socrates, 2004). The HMP-PPI complex spectrum reveals a shift of the lipid carbonyl peak as well as the absence of the 1390 cm^{-1} peak of PPI.

For all three complexes, their IR spectrum differentiated from that of their constituent biopolymers, suggesting thermodynamic compatibility between HMP and each of the proteins resulting in the development of intermolecular HMP-protein interactions.

4. Conclusions

The present work showed that coacervates composed of concentrated HMP and either SC, WPI or PPI systems can be formed by associative complexation under acidic conditions. However, the type of protein was important for the optimum coacervation conditions in terms of protein-HMP mixing ratio and pH. The selected isolated insoluble complexes of HMP with the three proteins, at the optimum coacervation conditions, showed lower solubility, greater moisture content, greater bulk and tapped densities, lower porosity and flowability, greater cohesiveness and inferior thickening ability than their constituents. Among the complexes, the PPI-HMP mixture showed a deviated behaviour compared to the other two complexes in several of the studied properties like solubility, moisture content, colour etc which were attributed to the weaker attractive forces between HMP and PPI. The findings of the present study can be a first step in the modulation of HMP based biopolymer complexes for future use as structuring or encapsulating agents in food matrices.

Author statement

Marianthi Zioga: Methodology, Investigation, Data curation.

Vasiliki Evageliou: Methodology, Resources, Supervision, Conceptualization, Writing - Original Draft, Writing- Reviewing and Editing.

Declaration of competing interest

The authors declare that they have no known competing financial interests or personal relationships that could have appeared to influence the work reported in this paper.

Data availability

The authors are unable or have chosen not to specify which data has been used.

Acknowledgements

The authors would like to thank Pr. I. Mandala (Agricultural University of Athens, Greece) for the zeta potential measurements. We are especially grateful to Pr. Chr. Pappas (Agricultural University of Athens, Greece) for the FT-IR experiments.

References

Anema, S. G., & de Kruif, C. G. (2014). Complex coacervates of lactotransferrin and β-lactoglobulin. *Journal of Colloid and Interface Science, 430*, 214–220. https://doi.org/10.1016/j.jcis.2014.05.036

Aryee, F. N. A., & Nickerson, M. T. (2012). Formation of electrostatic complexes involving mixtures of lentil protein isolates and gum Arabic polysaccharides. *Food Research International, 48*, 520–527. https://doi.org/10.1016/j.foodres.2012.05.012

Bédié, G., Turgeon, S., & Makhlouf, J. (2008). Formation of native whey protein isolate – low methoxyl pectin complexes as a matrix for hydro-soluble food ingredient entrapment in acidic foods. *Food Hydrocolloids, 22*, 836–844. https://doi.org/10.1016/j.foodhyd.2007.03.010

Bordón, M. G., Paredes, A. J., Camacho, N. M., Penci, M. C., Gonzalez, A., Palma, S. D., et al. (2021). Formulation, spray-drying and physicochemical characterization of functional powders loaded with chia seed oil and prepared by complex coacervation. *Powder Technology, 391*, 479–493. https://doi.org/10.1016/j.powtec.2021.06.035

Burger, T. G., & Zhang, Y.((2019). Recent progress in the utilization of pea protein as an emulsifier for food applications. *Trends in Food Science & Technology, 86*, 25–33. https://doi.org/10.1016/j.tifs.2019.02.007

Chegini, G., & Ghobadian, B. (2005). Effect of spray-drying conditions on physical properties of orange juice powder. *Drying Technology, 23*, 657–668. https://doi.org/10.1081/DRT-200054161

Dai, S., Jiang, F., Shah, N. P., & Corke, H. (2017). Stability and phase behavior of konjac glucomannan-milk systems. *Food Hydrocolloids, 73*, 30–40. https://doi.org/10.1016/j.foodhyd.2017.06.025

Devi, N., Sarmah, M., Khatun, B., & Maji, T. K. (2017). Encapsulation of active ingredients in polysaccharide-protein complex coacervates. *Advances in Colloid and Interface Science, 239*, 136–145. https://doi.org/10.1016/j.cis.2016.05.009

Duhoranimana, E., Yu, J., Mukeshimana, O., Habinshuti, I., Karangwa, E., Xu, X., et al. (2018). Thermodynamic characterization of gelatin–sodium carboxymethyl cellulose complex coacervation encapsulating conjugated linoleic acid (CLA). *Food Hydrocolloids, 80*, 149–159. https://doi.org/10.1016/j.foodhyd.2018.02.011

Espinosa-Andrews, H., Enriquez-Ramirez, K. E., Garcia-Marquez, E., Ramirez-Santiago, C., Lobato-Calleros, C., & Vernon-Carter, J. (2013). Interrelationship between the zeta potential and viscoelastic properties in coacervates complexes. *Carbohydrate Polymers, 95*, 161–166. https://doi.org/10.1016/j.carbpol.2013.02.053

Fitzpatrick, J. J., Iqbal, T., Delaney, C., Twomey, T., & Keogh, M. K. (2005). Effect of powder properties and storage conditions on the flowability of milk powders with different fat contents. *Journal of Food Engineering, 64*, 435–444. https://doi.org/10.1016/j.jfoodeng.2003.11.011

Frith, W. J. (2010). Mixed biopolymer aqueous solutions–phase behaviour and rheology. *Advances in Colloid and Interface Science, 61*, 48–60. https://doi.org/10.1016/j.cis.2009.08.001

Ghasemi, S., Jafari, S. M., Assadpour, E., & Khomeiri, M. (2017). Production of pectin – whey protein nano – complexes as carriers of orange peel oil. *Carbohydrate Polymers, 177*, 369–377. https://doi.org/10.1016/j.carbpol.2017.09.009

Gilsenan, P. M., Richardson, R. K., & Morris, E. R. (2003). Associative and segregative interactions between gelatin and low-methoxy pectin: Part 1. Associative interactions in the absence of Ca^{2+}. *Food Hydrocolloids, 17*, 723–737. https://doi.org/10.1016/S0268-005X(03)00094-8

Goff, H. D., & Guo, Q. (2019). The role of Hydrocolloids in the development of food structure. In F. Spyropoulos, A. Lazidis, & I. Norton (Eds.), *Handbook of food structure development* (pp. 1–28). The Royal Society of Chemistry. https://doi.org/10.1039/9781788016155-00001.

Guimarães, G. C., Coelho Júnior, M. C., & Garcia Rojas, E. E. (2009). Density and kinematic viscosity of pectin aqueous solution. *Journal of Chemical & Engineering Data, 54*, 662–667. https://doi.org/10.1021/je800305a

Hernández-Nava, R., López-Malo, A., Palou, E., Ramírez-Corona, N., & Jiménez-Munguía, M. T. (2020). Encapsulation of oregano essential oil (Origanum vulgare) by complex coacervation between gelatin and chia mucilage and its properties after spray drying. *Food Hydrocolloids, 109*, Article 106077. https://doi.org/10.1016/j.foodhyd.2020.106077

Hong, T., Iwashita, K., & Shiraki, K. (2018). Viscosity control of protein solution by small solutes: A review. *Current Protein & Peptide Science, 19*, 746–758. https://doi.org/10.2174/1389203719666171213114919

Hosseini, S. S., Khodaiyan, F., & Yarmand, M. S. (2016). Optimization of microwave assisted extraction of pectin from sour orange peel and its physicochemical properties. *Carbohydrate Polymers, 140*, 59–65. https://doi.org/10.1016/j.carbpol.2015.12.051

Huang, G. Q., Sun, Y. T., Xiao, J. X., & Yang, J. (2012). Complex coacervation of soybean protein isolate and chitosan. *Food Chemistry, 135*, 534–539. https://doi.org/10.1016/j.foodchem.2012.04.140

Jaya, S., & Das, H. (2004). Effect of maltodextrin, glycerol monostearate and tricalcium phosphate on vacuum dried mango powder properties. *Journal of Food Engineering, 63*, 125–134. https://doi.org/10.1016/S0260-8774(03)00135-3

Jinapong, N., Suphantharika, M., & Jamnong, P. (2008). Production of instant soymilk powders by ultrafiltration, spray drying and fluidized bed agglomeration. *Journal of Food Engineering, 84*, 194–205. https://doi.org/10.1016/j.jfoodeng.2007.04.032

Klemmer, K. J., Waldner, L., Stone, A., Low, N. H., & Nickerson, M. T. (2012). Complex coacervation of pea protein isolate and alginate polysaccharides. *Food Chemistry, 130*, 710–715. https://doi.org/10.1016/j.foodchem.2011.07.114

de Kruif, C. G., & Tuinier, R. (2001). Polysaccharide protein interactions. *Food Hydrocolloids, 15*, 555–563. https://doi.org/10.1016/S0268-005X(01)00076-5

Lan, Y., Chen, B., & Rao, J. (2018). Pea protein isolate - high methoxyl pectin soluble complexes for improving pea protein functionality: Effect of pH, biopolymer ratio and concentrations. *Food Hydrocolloids, 80*, 245–253. https://doi.org/10.1016/j.foodhyd.2018.02.021

Lan, Y., Ohm, J.-B., Chen, B., & Rao, J. (2020). Phase behavior and complex coacervation of concentrated pea protein isolate-beet pectin solution. *Food Chemistry, 307*, Article 125536. https://doi.org/10.1016/j.foodchem.2019.125536

Liu, S. H., Low, N. H., & Nickerson, M. T. (2009). Effect of pH, salt, and biopolymer ratio on the formation of pea protein isolate–gum Arabic complexes. *Journal of Agricultural and Food Chemistry, 57*, 1521–1526. https://doi.org/10.1021/jf802643n

Liu, J., Shim, Y. Y., Shen, Y., Wang, Y., & Reaney, M. J. T. (2017). Whey protein isolate and flaxseed (Linum usitatissimum L.) gum electrostatic coacervates: Turbidity and rheology. *Food Hydrocolloids, 64*, 18–27. https://doi.org/10.1016/j.foodhyd.2016.10.006

Liu, J., Shim, Y. Y., Wang, Y., & Reaney, M. J. T. (2015). Intermolecular interaction and complex coacervation between bovine serum albumin and gum from whole flaxseed (Linum usitatissimum L.). *Food Hydrocolloids, 49*, 95–103. https://doi.org/10.1016/j.foodhyd.2015.02.035

Li, Y., Zhang, X., Zhao, Y., Ding, J., & Lin, S. (2018). Investigation on complex coacervation between fish skin gelatin from cold-water fish and gum Arabic: Phase behavior, thermodynamic, and structural properties. *Food Research International, 107*, 596–604. https://doi.org/10.1016/j.foodres.2018.02.053

Matalanis, A., Lesmes, U., Decker, E. A., & McClements, D. J. (2010). Fabrication and characterization of filled hydrogel particle based on sequential segregative and aggregative biopolymer phase separation. *Food Hydrocolloids, 24*, 689–701. https://doi.org/10.1016/j.foodhyd.2010.04.009

Moschakis, T., & Biliaderis, C. G. (2017). Biopolymer-based coacervates: Structures, functionality and applications in food products. *Current Opinion in Colloid & Interface Science, 28*, 96–109. https://doi.org/10.1016/j.cocis.2017.03.006

Nep, E. I., & Conway, B. R. (2011). Physicochemical characterization of grewia polysaccharide gum: Effect of drying method. *Carbohydrate Polymers, 84*, 446–453. https://doi.org/10.1016/j.carbpol.2010.12.005

Opaliński, I., Chutkowski, M., & Hassanpour, A. (2016). Rheology of moist food powders as affected by moisture content. *Powder Technology, 294*, 315–322. https://doi.org/10.1016/j.powtec.2016.02.049

Pillai, P. K. S., Stone, A. K., Guo, Q., Guo, Q., Wang, Q., & Nickerson, M. T. (2019). Effect of alkaline de-esterified pectin on the complex coacervation with pea protein isolate under different mixing conditions. *Food Chemistry, 284*, 227–235. https://doi.org/10.1016/j.foodchem.2019.01.122

Plati, F., Ritzoulis, C., Pavlidou, E., & Paraskevopoulou, A. (2021). Complex coacervate formation between hemp protein isolate and gum Arabic: Formulation and characterization. *International Journal of Biological Macromolecules, 182*, 144–153. https://doi.org/10.1016/j.ijbiomac.2021.04.003

Raei, M., Rafe, A., & Shahidi, F. (2018). Rheological and structural characteristics of whey protein-pectin complex coacervates. *Journal of Food Engineering, 228*, 25–31. https://doi.org/10.1016/j.jfoodeng.2018.02.007

Ren, J.-N., Hou, Y.-Y., Fan, G., Zhang, L.-L., Li, X., Yin, K., et al. (2019). Extraction of orange pectin based on the interaction between sodium caseinate and pectin. *Food Chemistry, 283*, 265–274. https://doi.org/10.1016/j.foodchem.2019.01.046

Ricci, L., Umiltà, E., Righetti, M. C., Messina, T., Zurlini, C., Montanari, A., et al. (2018). On the thermal behavior of protein isolated from different legumes investigated by DSC and TGA. *Journal of the Science of Food and Agriculture, 98*(14), 5368–5377. https://doi.org/10.1002/jsfa.9078

Rocha, C. M. R., Souza, H. K. S., Magalhaes, N. F., Andrade, C. T., & Goncalves, M. P. (2014). Rheological and structural characterization of agar/whey proteins insoluble complexes. *Carbohydrate Polymers, 110*, 345–353. https://doi.org/10.1016/j.carbpol.2014.04.015

Ru, Q., Wang, Y., Lee, J., Ding, Y., & Huang, Q. (2012). Turbidity and rheological properties of bovine serum albumin/pectin coacervates: Effect of salt concentration and initial protein/polysaccharide ratio. *Carbohydrate Polymers, 88*, 838–846. https://doi.org/10.1016/j.carbpol.2012.01.019

Seerangurayar, T., Manickavasagan, A., Al-Ismaili, A. M., & Al-Mulla, Y. A. (2017). Effect of carrier agents on flowability and microstructural properties of foam-mat freeze dried date powder. *Journal of Food Engineering, 215*, 33–43. https://doi.org/10.1016/j.jfoodeng.2017.07.016

Shrestha, S., van't Hag, L., Haritos, V., & Dhital, S. (2023). Comparative study on molecular and higher-order structures of legume seed protein isolates: Lentil, mungbean and yellow pea. *Food Chemistry, 411*, Article 135464. https://doi.org/10.1016/j.foodchem.2023.135464

Socrates, G. G. (2004). *Infrared and Raman characteristic group frequencies: Tables and charts* (3rd ed.). John Wiley & Sons, Ltd.

Stenger, C., Zeeb, B., Hinrichs, J., & Weiss, J. (2017). Formation of concentrated biopolymer particles composed of oppositely charged WPI and pectin for food applications. *Journal of Dispersion Science and Technology, 38*, 1258–1265. https://doi.org/10.1080/01932691.2016.1234381

Synytsya, A., Čopíková, J., Matějka, P., & Machovič, V. (2003). Fourier transform Raman and infrared spectroscopy of pectins. *Carbohydrate Polymers, 54*, 97–106. https://doi.org/10.1016/S0144-8617(03)00158-9

Syrbe, A., Bauer, W. J., & Klostermeyer, H. (1998). Polymer science concepts in dairy systems–an overview of milk protein and food hydrocolloid interaction. *International Dairy Journal, 8*, 179–193. https://doi.org/10.1016/S0958-6946(98)00041-7

Timilsena, Y. P., Akanbi, T. O., Khalid, N., Adhikari, B., & Barrow, C. J. (2019). Complex coacervation: Principles, mechanisms and applications in microencapsulation. *International Journal of Biological Macromolecules, 121*, 1276–1286. https://doi.org/10.1016/j.ijbiomac.2018.10.144

Timilsena, Y. P., Wang, B., Adhikari, R., & Adhikari, B. (2016). Preparation and characterization of chia seed protein isolate–chia seed gum complex coacervates. *Food Hydrocolloids, 52*, 554–563. https://doi.org/10.1016/j.foodhyd.2015.07.033

Tolstoguzov, V. (2003). Some thermodynamic considerations in food formulation. *Food Hydrocolloids, 17*, 1–23. https://doi.org/10.1016/S0268-005X(01)00111-4

Turgeon, S. L., Schmitt, C., & Sanchez, C. (2007). Protein–polysaccharide complexes and coacervates. *Current Opinion in Colloid & Interface Science, 12*, 166–178. https://doi.org/10.1016/j.cocis.2007.07.007

Weinbreck, F., de Vries, R., Schrooyen, P., & de Kruif, C. G. (2003). Complex coacervation of whey protein and gum Arabic. *Biomacromolecules, 4*, 293–303. https://doi.org/10.1021/bm025667n

Weiss, J., Salminen, H., Moll, P., & Schmitt, C. (2019). Use of molecular interactions and mesoscopic scale transitions to modulate protein-polysaccharide structures. *Advances in Colloid and Interface Science, 271*, Article 101987. https://doi.org/10.1016/j.cis.2019.07.008

Yang, Y., Anvari, M., Pan, C. H., & Chung, D. (2012). Characterisation of interactions between fish gelatin and gum Arabic in aqueous solutions. *Food Chemistry, 135*, 555–561. https://doi.org/10.1016/j.foodchem.2012.05.018

Yücetepe, A., Yavuz-Düzgün, M., Şensu, E., Bildik, F., Demircan, E., & Özçelik, B. (2021). The impact of pH and biopolymer ratio on the complex coacervation of Spirulina platensis protein concentrate with chitosan. *Journal of Food Science and Technology, 58*, 1274–1285. https://doi.org/10.1007/s13197-020-04636-7

Zha, F., Dong, S., Rao, J., & Chen, B. (2019). Pea protein isolate-gum Arabic Maillard conjugates improves physical and oxidative stability of oil-in-water emulsions. *Food Chemistry, 285*, 130–138. https://doi.org/10.1016/j.foodchem.2019.01.151

Zha, F., Gao, K., Rao, J., & Chen, B. (2021). Maillard-driven chemistry to tune the functionality of pea protein: Structure characterization, site-specificity, and aromatic profile. *Trends in Food Science & Technology, 114*, 658–671. https://doi.org/10.1016/j.tifs.2021.06.029

Zhang, T., Xu, X., Li, Z., Wang, Y., Xue, Y., & Xue, C. (2018). Interactions and phase behaviors in mixed solutions of kappa-carrageenan and myofibrillar protein extracted from*Alaska Pollock*surimi. *Food Research International, 105*, 821–827. https://doi.org/10.1016/j.foodres.2017.11.080

Zhang, Y., & Zhong, Q. (2013). Encapsulation of bixin in sodium caseinate to deliver the colorant in transparent dispersions. *Food Hydrocolloids, 33*, 1–9. https://doi.org/10.1016/j.foodhyd.2013.02.009